RESEARCH

Improving Bond Performance of Near-Surface Mounted Steel Ribbed and Threated Rods in the Concrete

Sabry Fayed[1*], Emrah Madenci[2], Yasin Onuralp Özkiliç[2] and Mohamed H. Zakaria[1]

Abstract

In this study, the experimental findings of twenty pull-out tests on the bond efficiency of threaded/ribbed steel rods used in near-surface mounting (NSM) are presented. On a groove (20×20 mm) that was slotted in one of the sides of a concrete block measuring 250×250×200 mm, a pull-out experiment was performed. The primary factors are the slot-filling materials (substrate concrete and epoxy paste), bonded length (equal to 5, 7, 10, and 15 times the rod diameter), surface pattern conditions (conventional ribbed reinforcing rebar and threaded bolt), use of nuts or rings welded at the free end of the bonded length, and use of straight or spiral wire welded along the length of the bonded length. The tested specimens' ultimate bond strength, slip, bond stress–slip response, failure patterns, stiffness, and ductility are recorded and assessed. The results showed that the ultimate bond strength and corresponding slip of ribbed rods cemented with epoxy were higher by 11.11% and 199%, respectively, than those of ribbed rods submerged in the substrate. Over the controls, all NSM epoxy-rods exhibited a greater ductility. As the bonded length increased, the ultimate bond strength of NSM rods fell by 12–32%. As the bonded length increased, the stiffness decreased. On the other hand, the ductility of NSM epoxy-rods increased as the bonded length increased. All applied schemes such as nuts, rings, longitudinal bars, and spiral bars significantly improved the ultimate bond strength (maximum=25.93%) and corresponding slip (maximum=166.67%) of NSM threaded rods as compared to the control ones.

Keywords Near-surface mounted approach, Bond performance, Slip, Ribbed steel rods, Threaded steel rods, End anchorage, Surface features

1 Introduction

One of the most important ways used in strengthening of the structural elements is near-surface mounting (NSM). It requires placing external reinforcement rods or strips into precut concrete cover slots in the tension zone of the reinforced concrete (RC) flexural member or in the sides of element such as RC beams, columns or beam-column junctions, among other places. Using filler (epoxy adhesive), these NSM bars are fastened to the concrete surface within the slots. Previous researches on the effectiveness of NSM as flexural reinforcement (Abed et al., 2021; Abushanab et al., 2021; Attia et al., 2020; Dong et al., 2021; Liu et al., 2022; Wang et al., 2022), shear reinforcement (Abed et al., 2019; Al-Hamrani et al., 2021; Refai et al., 2022; Tomlinson & Fam, 2015), and compression reinforcement (Elmesalami et al., 2021; Elmessalami et al., 2019) for RC members had been reported, and it has been observed that this strengthening technique is well suited to improve and retrofit structural

*Correspondence:
Sabry Fayed
sabrielmorsi@yahoo.com; sabry_fayed@eng.kfs.edu.eg
[1] Civil Engineering Department, Faculty of Engineering, Kafrelsheikh University, Kafrelsheikh, Egypt
[2] Department of Civil Engineering, Necmettin Erbakan University, 42090 Konya, Turkey

performance of existing old elements. Because of their combination of high tensile strength and great ductility, deformed high strength steel bars are frequently utilized in the reinforcement of RC members as opposed to fibre reinforced polymer members, which experienced brittle failure. Moreover, the ribbed distortion of steel rods could offer strong anchoring and a high resistance to debonding. Tensile stress will rise as debonding is postponed and may eventually approach the bars' tensile strength.

The near-surface mounted (NSM) bar's ability to develop inside the groove greatly affects on how well it performs as extra reinforcement when strengthening preexisting RC elements. This is mostly influenced by the bar's surface properties, filler fracture characteristics and how they interact with the groove filler nearby (Novidis & Pantazopoulou, 2008). Composite of filling material (epoxy) and added-rod are referred to as a repair system (Lorenzis & Nanni, 2001). When NSM rods were placed at the concrete surface, both old reinforcement and new NSM rods are under same displacement conditions (Wang et al., 2022). In addition, NSM rods will aid the existing old reinforcing rods in carrying part of the force which led to increase in member capacity (Teng et al., 2006). The NSM bar's cylindrical contact surface with the surrounding filler and the groove's rectangular boundary with the surrounding concrete are the two interfaces where stress transmission and interaction take place. In both situations, load transfer is accomplished through friction for higher levels of slippage and chemical attachment for early phases of slip. If the employed bar has surface deformation, mechanical interlocking between the rebar and the filling material may happen (Novidis & Pantazopoulou, 2008). In general, almost failure patterns of pull out took placed at one of two contact surfaces (Novidis et al., 2007; Teng et al., 2006). As a result, bond strength could be controlled using surface properties of NSM rods, bonded length and end anchorages, which are the variables of the current paper.

The collapses types that can occur in the NSM pull-out test are: (1) splitting in the concrete, (2) shearing in the concrete, (3) pull out of NSM rod from epoxy which it was considered as ideal failure, and (4) split in the epoxy accompanied with or without concrete cracking around epoxy. Despite the advantages of reinforcing steel rods in terms of elongation compared to FRP rods, studies conducted on NSM steel rods are very few compared to those performed on NSM FRP rods. That might be the reason is the high tensile strength of the FRP material. This leads to a small cross-sectional area of the required rods, and thus a small area of grooves required on the concrete surface. But it is also important to use steel reinforcing rods that achieve high ductility and have full

compatibility with the concrete properties. Therefore, this study focuses on bond performance of NSM steel rods.

Many previous researches that related to NSM FRP bars examined the effects of slot dimension, rebar surface characteristics, rod diameter, embedded distance, epoxy type, and bond mechanism at rod-epoxy and concrete-epoxy interfaces (Al-Obaidi et al., 2018; Capozucca et al., 2015; Emara et al., 2018; Gomez et al., 2021; Cruz and Barros, 2002; Lee et al., 2013a; Lorenzis & Teng, 2007; Peng et al., 2015; Sharaky et al., 2013; Torres et al., 2016; Wang & Cheng, 2021a). It was noticed that slot size significantly affected the bond capacity of NSM rod (Sharaky et al., 2013). Additionally, an increase of 22% and 72% took placed in bond strength when rod diameter increased from 8 to 9 mm and from 8 to 12 mm, respectively. Due to the bar's roughened surface coming into touch with the epoxy matrix, sand-coated and corrugated NSM rods often offer good bond capacity (Lee et al., 2013a; Wang & Cheng, 2021a). According to Lee et al. (Lorenzis & Nanni, 2001), the use of spiral pattern and sand-coated NSM-GFRP as well as CFRP rebars demonstrated higher bond efficiency with respect to rebars with a smooth surface. These findings were corroborated by Wang and Cheng (Wang & Cheng, 2021b), who found that NSM-CFRP bars with spirally wrapped roughness and sand coating exceeded both roughened and sand-coated bars in terms of strength properties of the bond. On the opposite side, according to Soliman et al., 2011a, NSM-CFRP and GFRP rods attached to concrete using epoxy glue demonstrated a 40–56% increase in bonding in comparison to those attached using cementitious materials. Also, the researchers concluded that most samples with epoxy glue failed due to concrete splitting, while samples with cementitious materials failed due to adhesive splitting at the concrete-adhesive contact. Thus, using FRP rods with high tensile strength when NSM FRP rods were glued with epoxy adhesive is useless because concrete splitting will happen. As a result, high strength steel rods work well with epoxy adhesive, especially when the concrete beneath them has a normal compressive strength up to 30 MPa. It is well known that NSM strengthening methods are used to reinforce aged, weak concrete. In the current paper, the bond strength of NSM steel rods buried in ordinary concrete is investigated. This report attempts to increase bond strength using three crucial factors (bond length, type of steel bar either deformed steel or threaded steel rod, end stopper). Although there have been many studies on NSM FRP rods/strips (Al-Abdwais & Al-Mahaidi, 2016; Al-Mahmoud et al., 2011; Cruz & Barros, 2004a, 2004b; Kalupahana et al., 2013; Lorenzis & Teng, 2007; Peng et al., 2015; Wang & Cheng, 2021c; Zhu et al., 2018),

there are very few studies on NSM steel rods, particularly those that conduct end stoppers (end anchoring) at the bond length end.

Due to the bar's roughened texture coming into touch with the epoxy adhesive, sand-coated and ribbed NSM bars often provide strong bond strength (Wang & Cheng, 2021c). According to Lee et al. (2013b), the usage of spirally-wound and sand-coated NSM-GFRP and CFRP bars demonstrated improved bond performance in comparison to bars with a smooth surface. These findings were supported by Wang and Cheng (Wang & Cheng, 2021d), who also observed that NSM-CFRP bars with spirally wound texture and sand coating outperformed both roughened and sand-coated bars in terms of bond strength. On the other hand, according to Soliman et al. (Soliman et al., 2011b), NSM-CFRP and GFRP bars attached to concrete using epoxy adhesives demonstrated a 40–56% increase in bond strength in comparison to those attached using cementitious adhesives.

Previous researchers tried to perform the NSM pull-out test in two ways: the first is embedment of NSM rods on both opposite sides of the concrete block and the second is beam-pull out test. Disadvantages of the first way are: (1) The geometry of two NSM pull-out rods on both sides must be a perfect match to avoid any difference which is difficult, (2) The force transmitted to each rod must be exactly equal, (3) The failure took placed at each rod must be exactly match at the same time, and (4) flexural stresses resulted due to eccentricity caused flexural cracks with in bonded length. To avoid these matters, it is need to high cost, effort and time. Disadvantages of the second way are: (1) Unable to measure end-slip of NSM pull-out rod, (2) Unable to well see cracks spread and failure pattern and (3) sample size is relatively large which led to increase in cost. Based on analysis of previous investigations, it is must perform the following: (1) bonded length of NSM pull-out rod did not reach the concrete edges in pull out direction to avoid edge broken due to high shearing force at the concrete edge, and (2) concrete block size is large enough to avoid concrete splitting.

In the current paper, the bond strength of NSM steel bars is evaluated experimentally utilizing an eccentric pullout test specimen that has been adapted to address some of the drawbacks of traditional pull out bond experiments such as beam-pull out test or two NSM rods on two sides of the concrete block. The impact of the end stopper pattern, the bonded length, and the surface features of the bars, the three key technological criteria of this upgrading method, was investigated in a total of twenty tests. NSM bars were rods with a 10 mm diameter. Both normal deformed steel bars and threaded rods were performed.

2 Aims of the Study

Near-surface mounted (NSM) is the most current strengthening method for repairing reinforced concrete (RC) elements especially deficient in the shear and the flexure. Advantages of NSM rod construction are: not need surface preparing, except grooving, take little time for install, all required tools/materials are available, cheap and easy. This method becomes especially attractive to repair of decks/slabs at negative moments. There are many previous works studied application of NSM conventional ribbed reinforcing steel rods but NSM threated rods did not investigated before although threated rods are available, cheap, ease and fast in installation, and possibility of nuts fabrication as well as its high tensile strength. This study induced a realistic simulation of pull out test performed on NSM rods to avoid: (1) eccentricity between rod and applied pull out load, (2) flexure stresses within the bonded length, (3) fastening-mode collapse, (4) large size of tested sample, (5) difficulty of slip measure and (6) need to large embedded length. Moreover, presented studied sample can be well observed the behavior of bonded region during testing and slip-control mode was applied. During NSM process, it is possible to use a type of reinforcing bars with different surface patterns that give better bond to the slot-filling material (epoxy). In addition, it is possible to use different techniques (nuts, rings or longitudinal/spiral wires) that welded at the rebar surface to improve the bond between the bar and epoxy. Smaller diameters of NSM rods can be used for carrying a given specific tension force in case of improving bond strength then required size of grooving required for embedment will significantly reduce. So that, the studied parameters are: type of rod (surface pattern) either ribbed or threated rod, bonded length, using end buffers made from nuts and rings, using longitudinal/spiral wires. Besides that, referenced NSM rods were embedded in the substrate concrete samples before casting with same grooving geometry at the sample side to evaluate efficiency the techniques used in the current study.

3 Experimental Programme
3.1 Materials

Materials used in this work divided into three parts; substrate concrete of the blocks, NSM rebars and the epoxy. Twenty tested pull out samples were cast. As can be seen in Table 1, the concrete mixture included Portland cement with a 42.5 grade, water, graded crushed basalt dolomite with a maximum size of 15 mm, and sand as a fine aggregate. Mechanical sieve examination of the used basalt stone and sand is depicted in Fig. 1. Table 2 lists the physical characteristics of the components. The ratio of the water to the cement was

Fayed *et al. Int J Concr Struct Mater*   (2024) 18:3

Page 4 of 18

Table 1 The proportions of mix used (kg/m^3)

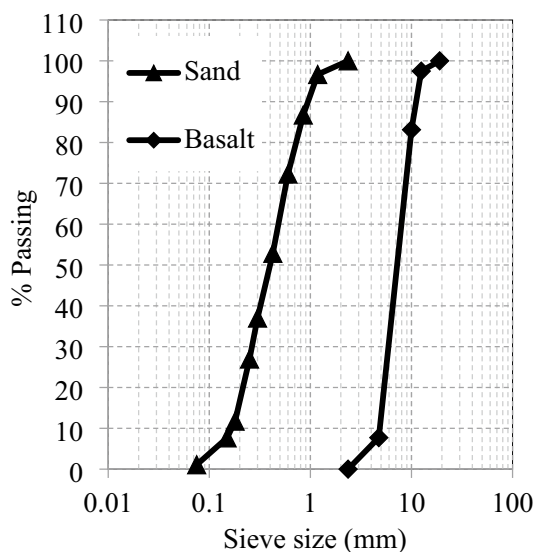| Water	Cement	Sand	Basalt dolomite
150	300	650	1290

Fig. 1 Particle size of sand and basalt used

0.5. The concrete mix's intended compressive strength was set at 25 MPa. To specify the compressive and the tensile strengths of the block concrete, three cubes and the cylinders were casted during blocks casting. After 28 days, the compressive and the tensile strengths were found 27 MPa, 2.5 MPa, respectively.

High tensile steel (HTS) and regular mild steel (NMS) were the types of the steel rebars used in this experiment. In contrast to HTS, which were 10 mm bars with either ribbed or threaded surfaces, NMS was a 2 mm wire with a smooth surface. Tension tests were performed to determine the mechanical properties of used steel bars. Fig. 2 depicts the stress–strain curves of the various bars. Elasticity modulus was around 200 GPa for three rods used. Yield/ultimate strengths and elongation were 250.3 MPa, 343.7 MPa and 34%, respectively, for 2 mm wire, 441.5 MPa, 537.5 MPa and 15.6%, respectively, for the ribbed rod, and were 529 MPa, 823.9 MPa and 17%, respectively, for the threaded rod.

Bar rib geometric features of the rebars utilized are important factor acting on the bond performance of rods. Fig. 3 shows all two types of rods used in the current work (ribbed deformed reinforced bar and threated rod). Both ribbed and threated rods had a deformation (spiral ribs) on its surface. Ribbed rod has a total diameter (d_e) and net diameter (d_b) of 11.1 mm and 9.5 mm, respectively. While difference between two diameters was 14.4%. For screw or threated bolt, d_e and d_b were 10.33 mm and 10 mm, respectively. Table 3 lists all measurements made on some rebars at various places as well as the average cross-sectional dimensions determined from those measurements. For simplifying, the bonded length was computed as a multiple of the rod diameter (Ø). Also, bond stress was computed based on the Ø. Moreover, groove size was based on the Ø.

The epoxy substance employed in this investigation was Sikadur 31CF (Data sheet of Sikadur 31CF). Rebars are bonded to concrete using this substance, which is described as a high strength epoxy resin. This epoxy has the benefits of not slumping, great strength, ease of usage, no requirement for primer material, and good chemical resistance. Additionally, it is utilized to adhere steel or carbon fibre strips to concrete. The product requires a 60–80 min initial cure and a 7 days service period, respectively. There were two parts to this epoxy: part A and portion B. Using a moderate speed drill, the two portions A and B were combined for two minutes, resulting in components with a consistent colour. The epoxy must be applied within 60 min of achieving the uniform colour because this is how long it takes for it to dry. The planted bars could be evaluated after 2 weeks of curing at 20 to 250 C in a room-temperature environment. Use of the lotion on wet skin or concrete is prohibited. Inside the groove, the concrete surface had been thoroughly cleaned.

Table 2 Physical features of materials used

Material	Maximum nominal size		Fineness modulus	Unit weight (kg/m^3)	Specific weight
	Diameter (mm)	Percentage (%)			
Basalt	15	2.51	2.11	1233.7	2.43
Sand	1.18	3.34	6.07	1302	2.67
Cement	0.075	13.8	NA	1206	3.13

Fayed *et al. Int J Concr Struct Mater*   (2024) 18:3
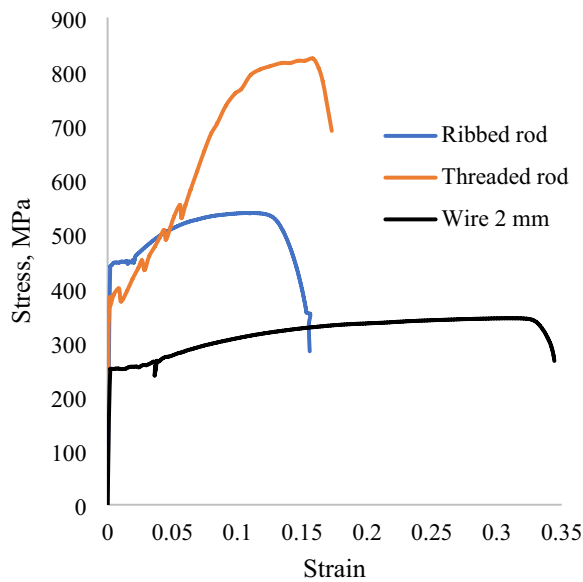
Page 5 of 18

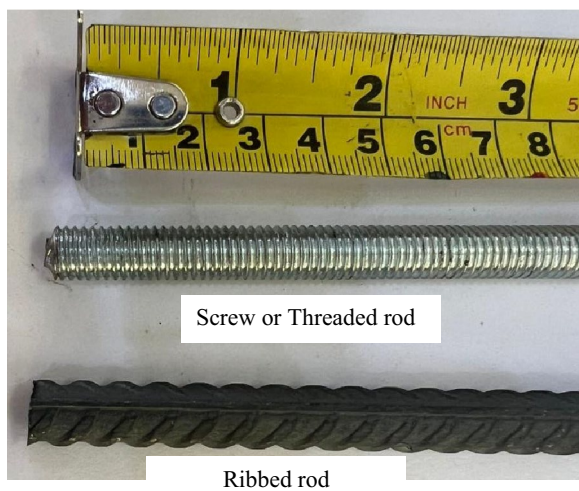
Fig. 2 Stress strain curves of bars used

Fig. 3 Types of steel rods used in the presented work

3.2 Preparing Substrate Concrete Blocks

Twenty similar substrate concrete blocks were prepared to use in embedment of NSM bar. Concrete block was cast inside specific form to give a U-shaped block. Cross-section of the block was 250×250 mm while height was 200 mm (Fig. 4). An inner hole of 100×100 mm was performed through whole height of the block. The hollow was positioned at the block side. Thick walls of 75 mm were conducted on two sides of the hollow to be strong during NSM process and during pull out test. A concrete specimen was cured in standard maintenance room for 56 days. Images of all samples pre/post casting are depicted in Fig. 5. Size of block was chosen to avoid occurrence of lateral cracks before bond collapse of NSM bar. This specimen has advantages such as a manageable specimen size, the ability to conduct the test in slip-control mode and quantify both the pull-out load and the end slip, and visual access to the test zone during loading. Moreover, this specimen limits the eccentricity problem, saves time of preparing before each test and saves material used in NSM process.

3.3 Test Variables Designation

Fig. 6 shows how to apply bond test of near-surface mounted (NSM) rod in concrete that performed in this work. Groove size was 20 mm width and 20 mm depth. It was selected to be equal 2 times the bar diameter ($\varnothing = 10$ mm). The block height (200 mm) was chosen larger than the longest bonded length ($15\varnothing = 150$ mm). Moreover, a distance between top concrete edge and bonded length was conducted to prevent occurrence of shear failure in concrete edge before bond failure particularly in case of the shortest bond length ($5\varnothing$). The experimental parameters were: slot-filling material (substrate concrete and epoxy paste), bonded length L_a (equal to 5, 7, 10 and 15 times the $\varnothing$), surface pattern condition (conventional ribbed reinforcing rebar and screw bolt), using nuts/rings welded at the free-end of the L_a and using straight/spiral wire welded within whole length of the L_b. Table 4 lists details of 20 specimens. Moreover, Fig. 7 depicts techniques used for enhancing bond strength of screw rods.

As shown in Table 4, first letter of the first six specimens was R, which refers to ribbed rod, while it was S for all rest ones, which refers to screw rod. Fourteen screw rods were strengthened at its surface using

Table 3 Surface characteristics of the rebars used

Type	Diameter Ø (mm)	Total diameter d_e (mm)	Net diameter d_b (mm)	$\frac{d_e - d_b}{d_b}$ (%)	Rib distance, S_r (mm)	Rib width, w_r (mm)	Rib height, h_r (mm)	Rib face angle (Degree)
Ribbed	10 mm	11.1	9.50	14.4	6	3.1	0.80	42.7
Threated	10 mm	10.33	10	3.3	1.67	1	0.17	80.8
Wire	2 mm	2	2	0	–	–	–	–

Ø is nominal diameter of the bar. d_e and d_b are the bar diameters with and without ribs, respectively
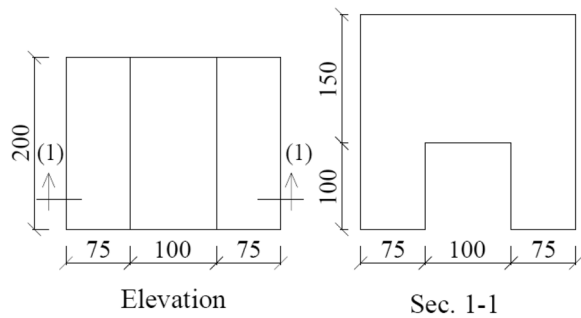
Fig. 4 Dimension of substrate concrete block, dim in mm

different techniques except two controls (S7ØE, with 7Ø bonded length and S0, with 5Ø bonded length). All specimens were divided into 8 groups to study effect of key variables. Group A consisted of three samples (R7ØN, R10ØN and R15ØN) which will examine effect of bonded length (7Ø, 10Ø and 15Ø) of ribbed (R) rods embedded in substrate normal concrete before casting. Positioning of these three rods was similar with that of rest rods in all twenty samples. Rest seventeen specimens were with epoxy-filled groove. Group B consisted of three samples (R7ØE, R10ØE and R15ØE) which will examine effect of bonded length (7Ø, 10Ø and 15Ø) of NSM ribbed (R) rods. Comparison between NSM specimen with epoxy-filled groove (R7ØE) and control one (R7ØN) was made in group C. In addition, group C included specimen S7ØE, with screw rod, to study effect of surface features on bond capacity. Group D included two specimens (S7ØE and S5ØE), which will examine effect of bonded length (5Ø and 7Ø) of NSM screw (S) rods. For simplifying, specimen S5ØE was labeled as S0 in Table 4. Group E (Fig. 7a) consisted of S0, S-1n5, S-2n5 and S-1n10. In this group,

one steel hexagonal nut (outside diameter = 17 mm and height = 5 mm) was fixed in S-1n5 while two steel hexagonal nuts (outside diameter = 17 mm and height = 5 mm) were fixed in S-2n5. S-1n10 had one steel hexagonal nut (outside diameter = 17 mm and height = 10 mm) at bond length end. In three groups (F, G and H), 2 mm wires were welded at screw rod surface to create obstacles that prevent and impede rod slipping. Group F (Fig. 7b) consisted of S0, S-1r, S-2r and S-3r. One, two and three rings, made from 2 mm wire, were fixed at end of bonded length in S-1r, S-2r and S-3r, respectively. Group G (Fig. 7c) consisted of S0, S-2b, S-3b and S-4b. Two, three and four longitudinal bars, made from 2 mm wire, were fixed along the bonded length in S-2b, S-3b and S-4b, respectively. In each specimen, longitudinal bars were uniformly distributed at outer diameter of rod to avoid any eccentricity during pull out test. Group H (Fig. 7d) consisted of S0, S-1s, S-2s and S-3s. One, two and three spirals,
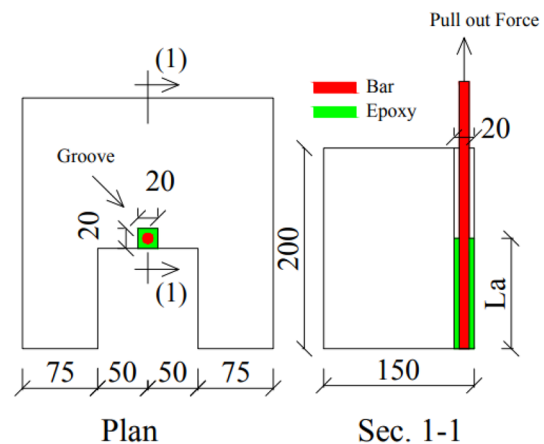

Fig. 6 Configuration of NSM method, dim in mm

(a) Samples before casting

(b) Samples after casting

Fig. 5 Preparing substrate concrete samples

Fayed *et al. Int J Concr Struct Mater*   (2024) 18:3

Page 7 of 18

Table 4 Samples' matrix

Specimen ID	Bar type	Filling material	L_a (times diameter)	d_b (mm)	Groove size	Description
R7ØN	Ribbed	Substrate normal concrete	**7Ø**	9.5	N/A	Ribbed bar embedded in normal concrete before casting ($L_a = $**7Ø**)
R10ØN	Ribbed	Substrate normal concrete	**10Ø**	9.5	N/A	Ribbed bar embedded in normal concrete before casting ($L_a = $10Ø)
R15ØN	Ribbed	Substrate normal concrete	**15Ø**	9.5	N/A	Ribbed bar embedded in normal concrete before casting ($L_a = $15Ø)
R7ØE	Ribbed	Epoxy	**7Ø**	9.5	20×20 mm	NSM ribbed bar ($L_a = $**7Ø**)
R10ØE	Ribbed	Epoxy	**10Ø**	9.5		NSM ribbed bar ($L_a = $10Ø)
R15ØE	Ribbed	Epoxy	**15Ø**	9.5		NSM ribbed bar ($L_a = $15Ø)
S7ØE	Screw	Epoxy	**7Ø**	10		NSM screw bar ($L_a = $**7Ø**)
S0 (Control)	Screw	Epoxy	5Ø	10		NSM screw bar ($L_a = $5Ø)
S-1n5	Screw	Epoxy	5Ø	10		NSM screw bar (Nut 5 mm)
S-2n5	Screw	Epoxy	5Ø	10		NSM screw bar (Two nuts 5 mm)
S-1n10	Screw	Epoxy	5Ø	10		NSM screw bar (Nut 10 mm)
S-1r	Screw	Epoxy	5Ø	10		NSM screw bar (One ring wire 2 mm)
S-2r	Screw	Epoxy	5Ø	10		NSM screw bar (Two rings wire 2 mm)
S-3r	Screw	Epoxy	5Ø	10		NSM screw bar (Three rings wire 2 mm)
S-2b	Screw	Epoxy	5Ø	10		NSM screw bar (Two longitudinal bar 2 mm along La)
S-3b	Screw	Epoxy	5Ø	10		NSM screw bar (Three longitudinal bar 2 mm along La)
S-4b	Screw	Epoxy	5Ø	10		NSM screw bar (Four longitudinal bar 2 mm along La)
S-1s	Screw	Epoxy	5Ø	10		NSM screw bar (one spiral wire 2 mm one loop and pitch = 50 mm = La)
S-2s	Screw	Epoxy	5Ø	10		NSM screw bar (Two spiral wire 2 mm two loop and pitch = 25 mm = La/2)
S-3s	Screw	Epoxy	5Ø	10		NSM screw bar (Three spiral wire 2 mm three loops and pitch = 16.7 mm = La/3)

made from 2 mm wire, were fixed along the bonded length in S-1s, S-2s and S-3s, respectively.

3.4 Constructing Near-Surface Mounted
Near-surface mounted (NSM) is a strengthening technique which is achieved by embedment of the steel bar by grooving the concrete surface to be reinforced in a specific direction. And this groove had specific width and depth. In the current investigation, a groove with Sect. 20×20 mm was saw using electrical ripsaw along the block height. Then, this slot was cleaned well using brush. The slot is filled partially (up to 50%) with epoxy, then the steel rod is positioned in the middle of the slot and pressed to force the epoxy to flow around the rod and completely fill all region between the rod and the slot. After that, the slot is completely filled with epoxy until the surface is leveled. Fig. 8 depicts NSM process of samples.

3.5 Pull Out Experiment
Fig. 9 shows testing setup used in this investigation. Pull-out experiments were carried out using a pullout hydraulic jack with a capacity of 200 kN. The displacement transducer was used to measure slip of the bar's loaded end. The applied load versus slip were documented. Moreover, cracking propagation and failure were observed during loading. The loading rate was 0.05 mm/min from beginning of loading to reach maximum bond stress while the rate was fast after the peak point.

## 4 Results
4.1 Cracks and Failures
Fig. 10 shows cracking and failures of tested samples while Table 5 summarizes failure modes. Fig. 10a–c depicts failures of ribbed rods embedded in normal substrate concrete (R7ØN, R10ØN and R15ØN). It is seen that failure of these samples is concrete cover splitting but as bonded length increased, cracks number and width of cracking zone, perpendicular on rod, increased. As a result, the pull-out load increased and corresponding slip declined with increase of bonded length. Fig. 10d–f depicts failures of NSM ribbed rods

Fayed *et al. Int J Concr Struct Mater*   (2024) 18:3

Page 8 of 18
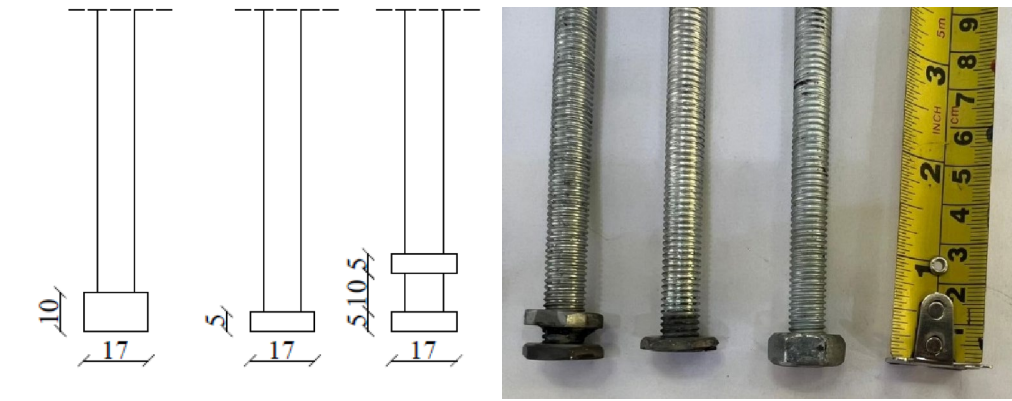
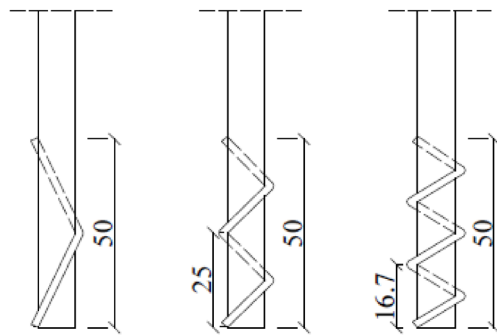**(a)** End nuts (S-1n5, S-2n5 and S-1n10); group E
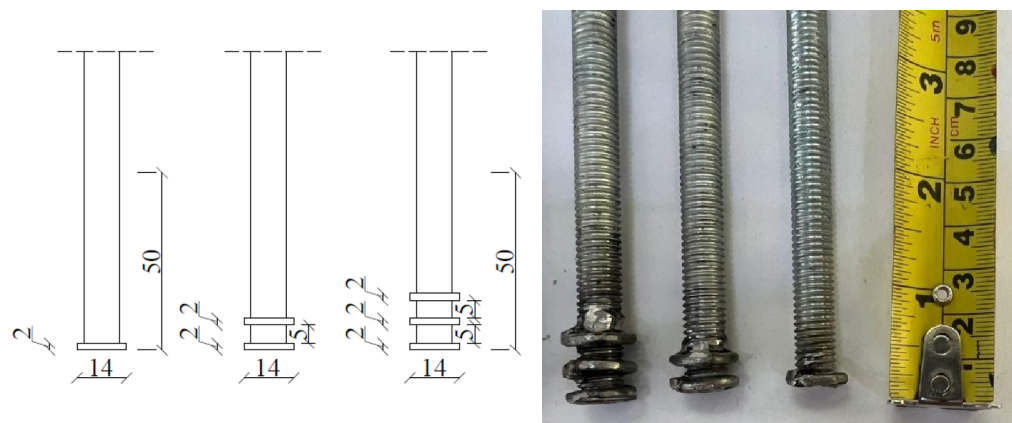
(b) 2 mm wire rings at the end (S-1r, S-2r, and S-3r); group F
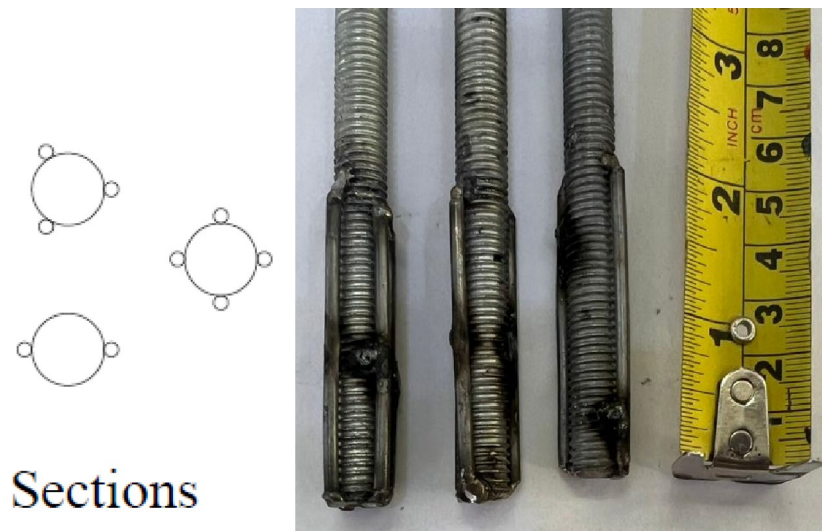
(c) 2 mm longitudinal wire (S-2b, S-3b, and S-4b); group G

Fig. 7 Details of pull out threaded rods used, dim in mm

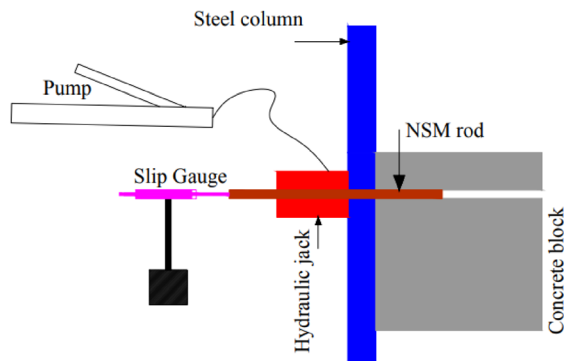**(d)** 2 mm spiral wire (S-1s, S-2s, and S-3s); group H

Fig. 7 continued

Fig. 8 NSM process of samples

(R7ØE, R10ØE and R15ØE) glued with epoxy which had same bonded lengths of three control specimens (R7ØN, R10ØN and R15ØN). For three specimens (R7ØE, R10ØE and R15ØE), one hair splitting crack occurred along bonded length but it did not cause the failure. In other words, debonding between rod and epoxy did not took place. Epoxy can transfer the pull-out force to the surrounding concrete and the split occurred in the concrete outside the groove area. R7ØE, R10ØE were failed at epoxy-concrete interface accompanied by splitting and shearing of concrete body (failure mode II). As a result of distributing the pull-out force over an area more than groove region, the three epoxy-glued samples (R7ØE, R10ØE and R15ØE) achieved loads more than those of the corresponding ones (R7ØN, R10ØN and R15ØN). The shorter the bonded length (R10ØN), the more this leads to distributing the load over a shorter distance from the concrete and causing a part of the concrete to be withdrawn (Fig. 10e). Conversely, the greater bonded length is better and does not cause shearing of the concrete (Fig. 10f). As shown in Fig. 10g, failure of specimen

S7ØE, with threaded rod, is debonding epoxy at groove edges. Nearly, two specimens S7ØE and R7ØE achieved same failure pattern and capacity. R15ØE, S7ØE were failed at epoxy-concrete interface then hair split in epoxy occurred then rupture of the concrete at the block edge without splitting of concrete body happened (failure mode III). Fig. 10h shows failure of specimen S0, with threaded rod and with $L_b = 5Ø$ without strengthening schemes. It cracked outside groove and the surrounding concrete was cracked. Due to decline of bonded length in this specimen compared to S7ØE, the failure was dangerous where a part of the concrete was withdrawn. All rest samples were failed at the concrete surrounding the groove accompanied or not by split in the epoxy (mode IV).

Fig. 10m–l shows failures of specimens S-1n5, S-2n5 and S-1n10 where it was similar to that of S0 but clear debonding occurred at rod end due to using end nuts. Fig. 10o-k show failures of specimens S-1r, S-2r and S-3r where it was similar to that of S0 except clear debonding occurred at rod end in specimen S-3r which three rings worked as end nut. It was observed as rings

(a) Testing set up

(b) Front view

(c) Back view

Fig. 9 Pull out test

$$\tau = \frac{P}{\pi \emptyset L_b} \tag{1}$$

where L_b is the bond length and $\emptyset$ is the bar diameter.

The bond stress–slip graphs for each pull out specimen are shown in Fig. 11. The bond stress–slip behaviour of NSM rods is often marked by an early bond stress rise with minimal slip, subsequently accompanied by softening once the maximum stress occurs. According to the pullout assessment findings, the local bond stress–slip chart can be divided into the following stages: stage I: Because of the chemical bonding process between the rod and the epoxy, there is a brief non-slip straight line length. Stage II: The chemical bond between the rod and the concrete/epoxy breaks down, causing the rod and concrete/epoxy to start sliding about within one another. Stage III: The curve peaks when the load rises and the bond stress reaches the splitting bond strength. Stage IV: As a result of shearing or splitting in the concrete near the groove, the bond stress is fast reducing while the slippage is rapidly growing.

In general, there is no remarkable difference in bond exhibition between rods embedded in concrete (group A) and NSM epoxy-rods (group B) in ascending and descending branches. In ascending phase, it was seen that slip growth of rods embedded in concrete was smaller than that of NSM epoxy-rods due to chemical bond between rod and cement mortar is stronger that of chemical bond between rod and epoxy mortar as well as coarse aggregate of concrete increased the shear resistance of concrete more than epoxy mortar. As shown in Fig. 11c, stiffness of R7ØN was larger than R7ØE as well as length of descending branch of R7ØN was longer and softened due to friction between rod and concrete while failure of R7ØE occurred at epoxy-concrete interface. By comparing two samples R7ØE and S7ØE, it is seen that remarkable difference happened when surface features changed from conventional ribbed and threaded rods. There were little increases in initial slip when bonded length increased from 5Ø to 7Ø to 10Ø to 15Ø (group A, B and D). although this is considered as negative effect, some samples (R15ØE and S7ØE) achieved high ductility when bonded length increased. From Fig. 11e–f, it was shown that the slip rate at the same bond stress level increased as number of nuts/rings raised. This may have happened because the nuts/rings were put at the end of the rod, which concentrated bond stress and caused a rapid failure. The slip rate of NSM rods provided with deformations schemes at various levels of bond stresses was comparable to control NSM rod (S0) with no scheme when longitudinal or spiral wires were welded on the rod surface (Fig. 11g–h). It was noted that spiral systems
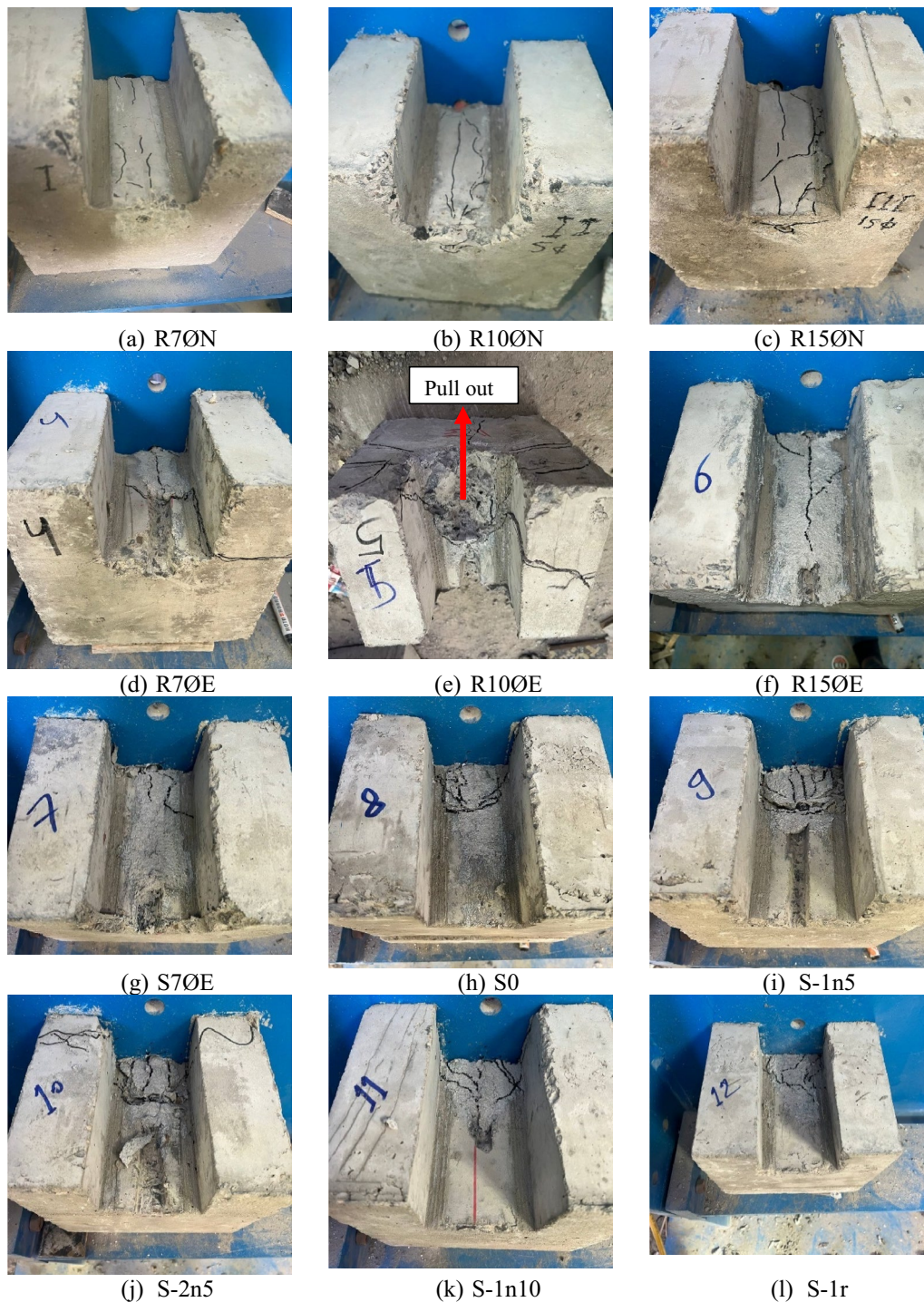
number increased, cracks increased and it spreads at larger area. Fig. 10s-u and v-y depict failures of specimens provided with longitudinal wires (S-2b, S-3b and S-4b) and specimens provided with spirals (S-1s, S-2s and S-3s). It showed that as number of longitudinal or spirals increased, bonding between rod and epoxy increased, hence cracking spread more.

4.2 Bond Stress–Slip Response

During the pullout test, adhesion and mechanical bonding transfer load from the NSM rod to the surrounding concrete or epoxy. The mechanical bond is created by the rod studs bearing against the surrounding filling material. This is the most typical load transmission method, and splitting of the surrounding concrete or epoxy is frequently used to control its strength limit condition. Measurements of the imposed pull out load (P) and the corresponding slip (δ) were taken. The following approach, which assumes that the bond stresses are evenly distributed along the bonded length, was used to compute the local bond stress (τ):

Fayed *et al. Int J Concr Struct Mater*   (2024) 18:3

Page 11 of 18

(a) R7ØN

(b) R10ØN

(c) R15ØN

(d) R7ØE

(e) R10ØE

(f) R15ØE

(g) S7ØE

(h) S0

(i) S-1n5

(j) S-2n5

(k) S-1n10

(l) S-1r

Fig. 10 Failure modes of tested pull out NSM specimens

provide the best comparability in this situation. Spiral wire is, therefore, the best design among all investigated approaches.

When the bonding resistance between the concrete and the NSM rod surpasses the maximum permissible value for reinforced concrete structures, both the NSM bar and the substrate concrete collectively lose their ability to resist forces from the outside. The specimens' final bond stress can be utilized to determine if the bond qualities are good or bad. The effect of
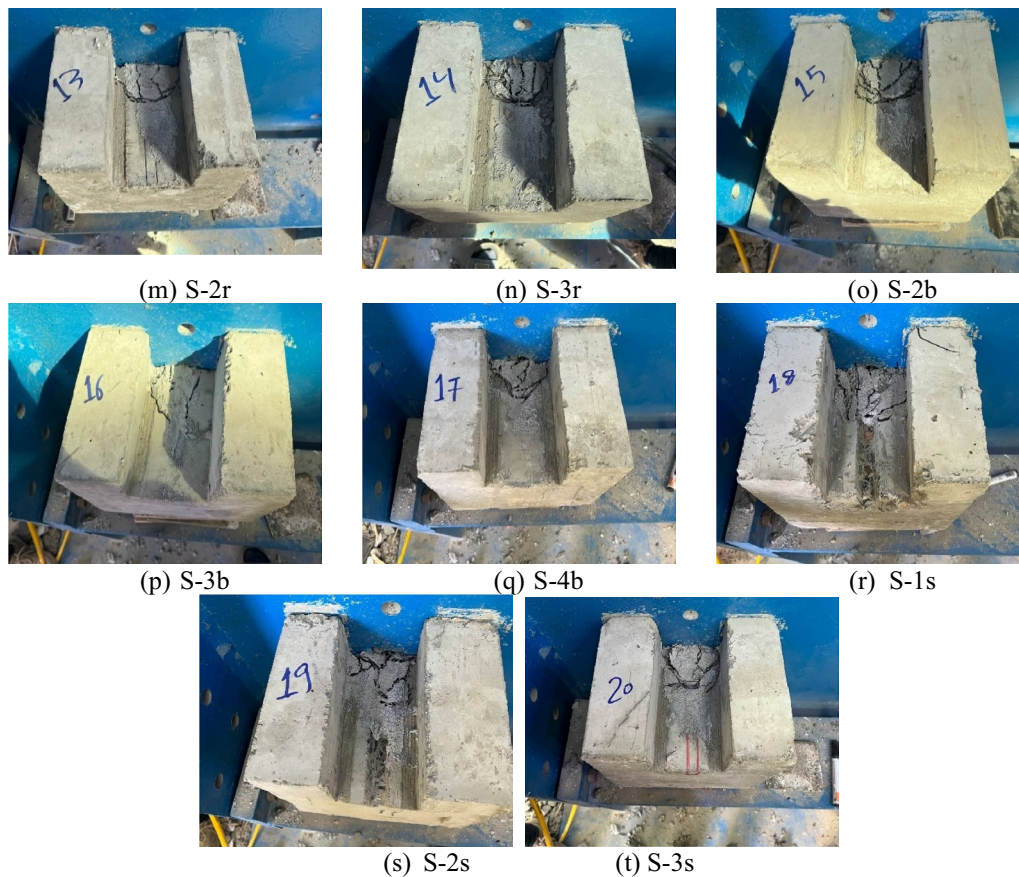
(m) S-2r   (n) S-3r   (o) S-2b

(p) S-3b   (q) S-4b   (r) S-1s

(s) S-2s   (t) S-3s

Fig. 10 continued

Table 5 Failures of tested specimens

Mode	Description	Specimens
I	Failed at rod-substrate concrete interface accompanied by splitting of concrete cover along bonded length	R7ØN, R10ØN, R15ØN
II	Failed at epoxy-concrete interface accompanied by splitting and shearing of concrete body	R7ØE, R10ØE
III	Failed at epoxy-concrete interface then hair split in epoxy then rupture of the concrete at the block edge without splitting of concrete body	R15ØE, S7ØE
IV	Failed at the concrete surrounding the groove accompanied or not by split in epoxy	S0, S-1n5, S-2n5, S-1n10, S-1r, S-2r, S-3r, S-2b, S-3b, S-4b, S-1s, S-2s, S-3s

unequal distribution bar embedment length on bond stress may be ruled out, particularly for a local bond. In other words, the comparison result of local bond testing is more usual. Table 6 displays the ultimate bond strength and its corresponding slip results for all samples. Also, stiffness and toughness were obtained from bond stress–slip curves and are listed in Table 6. It is important to know the effect of studied parameters on both rigidity and ductility of bond response. It is well known that stiffness and toughness are indicators for rigidity and ductility, respectively. In this study, stiffness (k) is estimated by dividing value of 0.5 τu on its corresponding slip. While toughness (T) is estimated by total area under bond stress–slip curve between original and peak point. In the following sections, effect of key parameters on τu, δu, k and T will discuss.
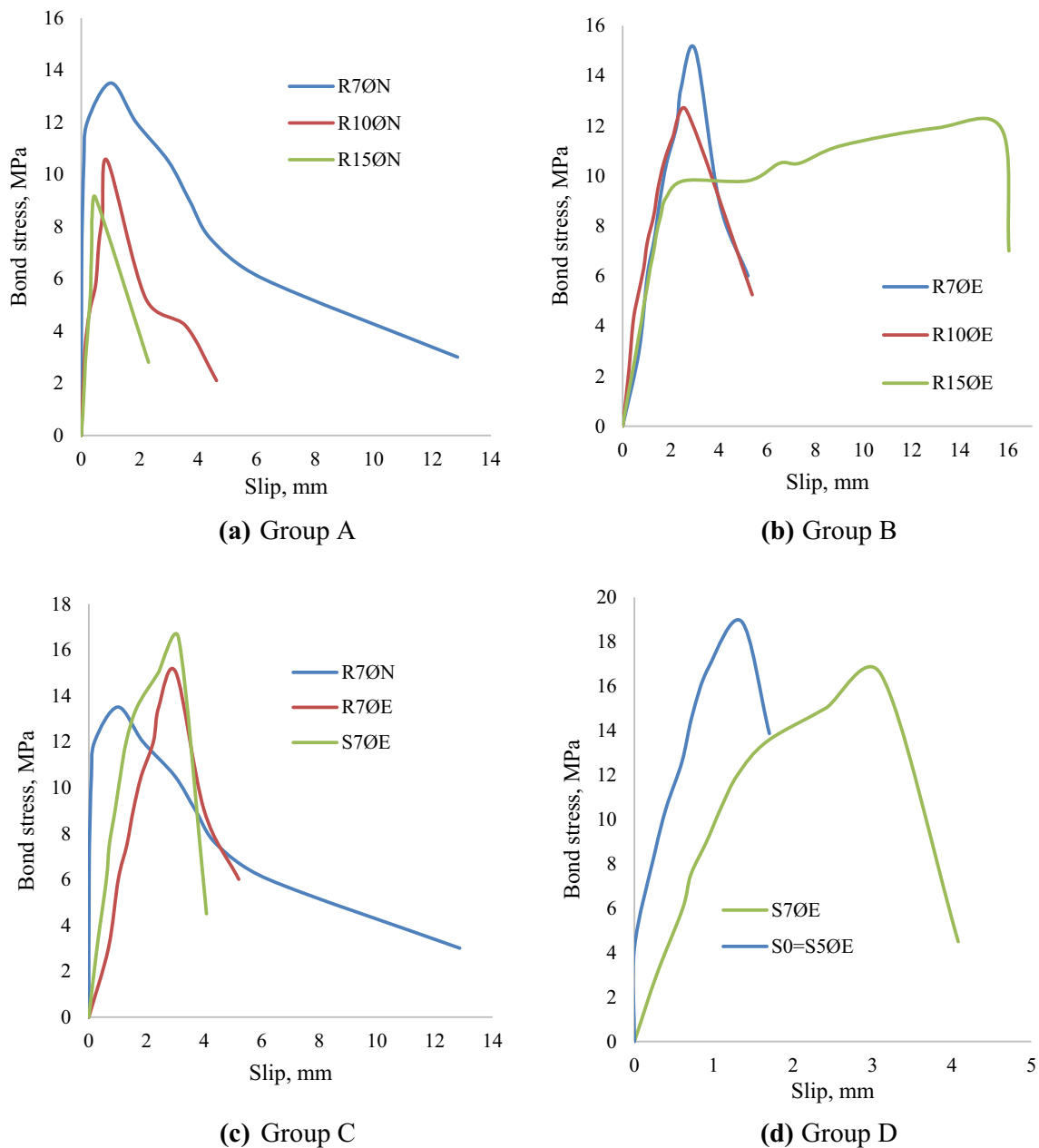
Fig. 11 Bond stress–slip curves of all tested groups

4.3 Ultimate Bond Strength and Corresponding Slip

In general, it was noticed that ultimate bond strength (τ_u) of all NSM rods, with different schemes, that were glued with groove-filling material (epoxy), were higher than that of rods embedded in substrate concrete (R7ØN, R10ØN, R15ØN). Also, almost epoxy-NSM rods achieved ultimate slip (δ_u) larger than those of specimens R7ØN, R10ØN, and R15ØN showing positive effect on both capacity and deformability of bond response. τ_u and δ_u of epoxy-rod sample (R7ØE) were 11.11% and 199%, respectively, higher than those of rod embedded in substrate (R7ØN). This occurred due to bond strength of the epoxy used in this work was higher than that of the substrate concrete which led to transfer failure from rod-concrete interface (R7ØN, R10ØN, R15ØN) into epoxy-concrete interface (rest samples). Hence, friction area was larger in case of epoxy-concrete interface compared to rod-concrete interface which enhanced the bond performance (increase in τ_u and δ_u).
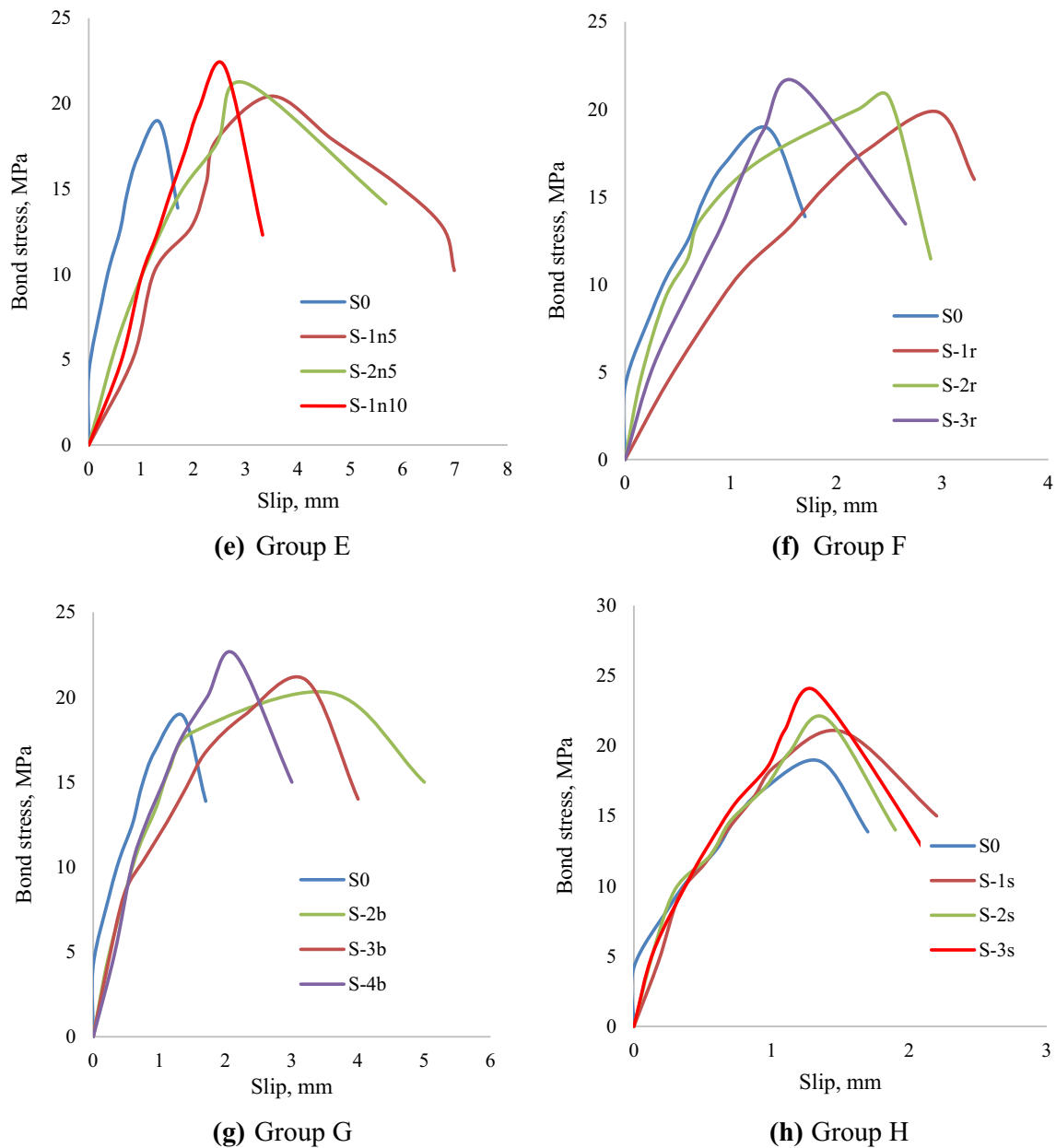
(e) Group E

(f) Group F

(g) Group G

(h) Group H

Fig. 11 continued

Effect of the bonded length (L_b) on the τu and the δu was studied in groups A, B and D. It was noticed that as the L_b increased, the τu declined. For the ridded rods, the τu of R15ØN, with $L_b = 15Ø$, was 32.59% less than that of R7ØN, with $L_b = 7Ø$. τu of R15ØE, with $L_b = 15Ø$, was 20.67% less than that of R7ØE, with $L_b = 7Ø$. For the threaded rods, the τu of S7ØE, with $L_b = 7Ø$, was 12.70% less than that of S5ØE (S0), with $L_b = 5Ø$. The reason was unequal distribution of the bond stress along bonded length where the maximum

value took placed at the start (loaded end) and minimum value occurred at free unloaded end of the L_b. As the bonded length was shorter (local bond), the uniform bond distribution occurred hence the bond capacity of the NSM rod will be larger. It was noticed that as the L_b increased, the ultimate slip declined in case of rods embedded in the substrate concrete (R7ØN, R10ØN, R15ØN) while it increased in case of the epoxy-rods. This occurred due to friction area was

Fayed *et al. Int J Concr Struct Mater*   (2024) 18:3

Page 15 of 18

Table 6 Results of pull out tests

Specimen ID	τu (Mpa)	Gain in τu (%)	δu (mm)	Gain in δu (%)	Stiffness k (MPa/mm)	Gain in k (%)	Toughness T (MPa.mm)	Gain in T (%)
Bonded length impact of ribbed rods embedded in substrate concrete; group A								
R7ØN	13.5	0.00	1.01	0.00	60.05	0.00	13.00	0.00
R10ØN	10.5	− 22.22	0.9	− 10.89	23.10	− 61.53	4.73	− 63.65
R15ØN	9.1	− 32.59	0.49	− 51.49	22.50	− 62.53	2.23	− 82.85
Bonded length impact of NSM ribbed rods; group B								
R7ØE	15	0.00	3.02	0.00	5.90	0.00	22.65	0.00
R10ØE	12.6	− 16.00	2.65	− 12.25	6.80	15.25	16.70	− 26.29
R15ØE	11.9	− 20.67	15.71	420.20	5.40	− 8.47	115.00	407.73
Filling epoxy/surface pattern impact of NSM rods; group C								
R7ØN	13.5	0.00	1.01	0.00	60.05	0.00	13.00	0.00
R7ØE	15	11.11	3.02	199.01	5.90	− 90.17	22.50	73.08
S7ØE	16.5	10*	3.11	2.98*	10.10	71.2*	25.70	14.22*
Bonded length impact of NSM threaded rods; group D								
S0 = S5ØE	18.9	0.00	1.35	0.00	24.30	0.00	12.76	0.00
S7ØE	16.5	− 12.70	3.11	56.60	10.10	− 58.40	25.66	101
End nuts impact of NSM threaded rods; group E								
S0	18.9	0.00	1.35	0.00	24.30	0.00	12.76	0.00
S-1n5	20.4	7.94	3.5	159.26	6.10	− 74.90	35.70	179.78
S-2n5	21.17	12.01	3	122.22	9.50	− 60.91	31.76	148.86
S-1n10	22.1	16.93	2.6	92.59	9.55	− 60.70	28.73	125.16
End rings impact of NSM threaded rods; group F								
S0	18.9	0.00	1.35	0.00	24.30	0.00	12.76	0.00
S-1r	19.8	4.76	2.95	118.52	9.50	− 60.91	29.21	128.92
S-2r	20.6	8.99	2.5	85.19	24.20	− 0.41	25.75	101.84
S-3r	21.55	14.02	1.63	20.74	15.40	− 36.63	17.56	37.67
Longitudinal bars impact of NSM threaded rods; group G								
S0	18.9	0.00	1.35	0.00	24.30	0.00	12.76	0.00
S-2b	20.2	6.88	3.6	166.67	17.20	− 29.22	36.36	185.01
S-3b	21.17	12.01	3.21	137.78	18.10	− 25.51	33.98	166.34
S-4b	22.49	18.99	2.14	58.52	17.90	− 26.34	24.06	88.63
Spiral bars impact of NSM threaded rods; group H								
S0	18.9	0.00	1.35	0.00	24.30	0.00	12.76	0.00
S-1 s	20.98	11.01	1.52	12.59	25.50	4.94	15.94	24.98
S-2 s	21.9	15.87	1.4	3.70	26.10	7.41	15.33	20.16
S-3 s	23.8	25.93	1.33	− 1.48	26.40	8.64	15.83	24.06

* Is referred to that the control specimen is R7ØE

larger in case of the epoxy-concrete interface compared to the rod-concrete interface.

At a specific $L_b = 7Ø$ (group C), it was found that both τu and δu of conventional ribbed rod and threaded rod are identical, approximately, showing possibility of using threaded rods in NSM method instead of conventional ribbed rods with same efficiency. Advantages of these threaded rods are possibility of using nuts as end stopper (anchorage) as well as, its high tensile strength.

It is was observed that all used schemes [nuts (group E), rings (group F), longitudinal bars (group G) and spiral bars (group H)] significantly improved ultimate bond strength (maximum = 25.93%) and corresponding slip (maximum = 166.67%) of NSM threaded rods. Using nuts with different sizes worked as stopper prevented and delayed rod slippage as well as increase rod-epoxy interface hence led to improve bond response. Same effect occurred when multi rings were welded at end of rod. As amount of nuts/rings increased, bond strength improved more. Surface features of NSM rods had a clear positive effect on bond response so studying use of additional deformations on the rod surface is important variable.

In group G, using two, three and four longitudinal bars that welded on rod surface increased the τu by 6.8, 12 and 18.99%, respectively. In group H, using one, two and three spiral bars that welded on rod surface increased the τu by 11, 15.87 and 25.93%, respectively. It was showed that as deformations increased, bond strength improved more. It was found that ultimate slip declined as deformations (nuts, rings, longitudinal bars and spiral bars) increased because of these deformations increased restriction of rod slippage.

4.4 Bond Stiffness

In general, it was noticed that stiffness (k) of almost NSM epoxy-rods were smaller than that of rods embedded in substrate concrete (R7ØN, R10ØN, R15ØN). The k of epoxy-rod sample (R7ØE) were 90.17% less than that of rod embedded in substrate (R7ØN). In general, it was known that first phases of bond stress–slip relationship of rod embedded in concrete are: (1) stage I: due to the chemical bonding action between the bar and concrete, there is a short non-slip straight line segment during the initial loading time, and (2) stage II: when the load reaches 30% of the maximum bond stress, the chemical bonding action between the rod and concrete doesn't work, and the rod and concrete begin to move relative to one another (Fayed, et al., 2023). This slippage behavior did not occur in epoxy-rod sample because slip took placed at epoxy-concrete interface. Moreover, the chemical bonding action between epoxy and old substrate concrete was less than that of rod-concrete interface.

It was noticed that as L_b increased, k declined for almost samples. For ridded rods, k of R15ØN, with $L_b = 15$Ø, was 62.5% less than that of R7ØN, with $L_b = 7$Ø. For threaded rods, τu of S7ØE, with $L_b = 7$Ø, was 58.4% less than that of S5ØE, with $L_b = 5$Ø. Showing initial slippage rate of short bonded length was less that of long bonded length. The reason was unequal distribution of bond stress along bonded length. It was found that k of threaded rod (S7ØE) was 71.2% larger than that of the conventional ribbed rod (R7ØE) showing possibility of using threaded rods in NSM method.

It is was observed that almost used schemes (nuts, rings, longitudinal bars) had a negative impact (maximum decline = 74%) on bond stiffness while spiral bars (group H) slightly improved bond stiffness (maximum = 8.64%). Using end stopper (nuts or rings) increased initial slippage rate compared to spiral bars (surface features). It was might be due to end stopper increased stress concentration at small distance and caused weakness in epoxy-concrete interface hence slippage rate at the loading start growth quickly. Based on the results, it is recommended in making the spiral bars scheme because it improves both ultimate bond strength, ultimate slip and stiffness of NSM threaded rods.

4.5 Ductility

Ductility of samples was estimated by bond toughness (T) which is listed in Table 6. In general, it was noticed that bond toughness (T) of all NSM epoxy-rods, except S0, were larger than that of rods embedded in substrate concrete (R7ØN, R10ØN, R15ØN). It is notably that sample S0 had L_b equal 5 times rod diameter which less that L_b of three samples R7ØN, R10ØN, R15ØN. It is can said that ductility of all NSM epoxy-rods was larger than controls. As listed in the results, the T of epoxy-rod sample (R7ØE) was 73% higher than that of rod embedded in substrate (R7ØN). Slippage occurred in epoxy-rod samples epoxy-concrete interface (larger friction area) while it took placed at rod-epoxy interface (smaller friction area) in R7ØN.

It was noticed that as L_b increased, ductility declined for rods embedded in substrate concrete. T of R15ØN, with $L_b = 15$Ø, was 82.8% less than that of R7ØN, with $L_b = 7$Ø. On the other hand, the ductility of NSM epoxy-rods increased as L_b increased. T of R15ØE, with $L_b = 15$Ø, was 407% larger than that of R7ØE, with $L_b = 7$Ø. For threaded rods, T of S7ØE, with $L_b = 7$Ø, was 101% larger than that of S5ØE, with $L_b = 5$Ø. It was found that T of threaded rod (S7ØE) was 14.22% larger than that of the conventional ribbed rod (R7ØE) showing possibility of using threaded rods in NSM method without any loss in the ductility.

It is was observed that all used schemes (nuts, rings, longitudinal/spiral bars) for improving bond response had a significantly impact (maximum gain = 185%) on bond ductility. T of S-1n5, S-2n5 and S-1n10 was 179.78, 148.86 and 125.16%, respectively, referenced to control sample (S0) with no nuts. T of S-1r, S-2r and S-3r was 128.92, 101.84 and 37.67%, respectively, referenced to control sample (S0) with no rings. Demonstrating that all schemes increased carrying loads and its corresponding slips hence led to improving bond ductility.

5 Conclusion

Near-surface mounting (NSM) is one of the most significant methods for strengthening forced concrete elements. The primary focus of this work is the bond performance of NSM steel rods either ribbed or threaded type. On a concrete block with the dimensions $250 \times 250 \times 200$ mm, a pull-out experiment was run. A 20 mm wide by 20 mm deep groove was slotted at the block side to facilitate NSM rod embedment. Traditional ribbed and threaded rods, both with a diameter of 10 mm, are the two types of rods used. The maximum strength and elongation of threaded rod were 823.9 MPa

and 17%, compared to 537.5 MPa and 15.6% for ribbed rod. NSM ribbed/threaded steel bars were cemented with groove filler (epoxy), as opposed to ribbed steel bars that were buried in the concrete before casting. The primary factors are the slot-filling materials (substrate concrete and epoxy paste), bonded length (equal to 5, 7, 10, and 15 times the rod diameter), surface pattern conditions (conventional ribbed reinforcing rebar and threaded bolt), use of nuts or rings welded at the free end of the bonded length, and use of straight or spiral wire welded along the length of the bonded length. The tested specimens' ultimate bond strength, slip, bond stress–slip response, failure patterns, stiffness, and ductility are recorded and examined. The outcomes are shown as follows:

1. The ultimate bond strength and corresponding slip of ribbed rods coated with epoxy were higher by 11.11% and 19%, respectively, than those of ribbed rods submerged in substrate. Epoxy rods that are nearly NSM have less rigidity than rods that are submerged in concrete. All NSM epoxy-rods, in contrast, were more ductile than the controls.
2. As the bonded length increased from 7 to 15 times the rod diameter, the ultimate bond strength of ribbed rods buried in concrete reduced by 32.59%. The ultimate bond strength of ribbed rods cemented with epoxy dropped by 20.67% as the bonded length increased from 7 to 15 times the rod diameter. Almost all samples showed a reduction in stiffness as the bonded length increased. Rod ductility declined with bond length for those placed in substrate concrete. On the other hand, the ductility of NSM epoxy-rods increased as the bonded length increased.
3. The potential of employing threaded rods in NSM method instead of regular ribbed rods with the same efficiency is demonstrated by the fact that both ultimate bond strength and corresponding slip of conventional ribbed rod and threaded rod are roughly equivalent as well as its stiffness was enhanced by 71.2%.
4. The ultimate bond strength (maximum = 25.93%) and corresponding slip (maximum = 166.67%) of NSM threaded rods were dramatically increased by all employed schemes nuts, rings, longitudinal bars, and spiral bars as compared to control ones. Additionally, the bond stiffness was negatively impacted by practically all schemes (nuts, rings, and longitudinal bars) (highest decline = 74%), but spiral bars marginally increased bond stiffness (maximum improvement = 8.64%). All employed bond response improvement techniques greatly improved bond ductility (highest gain = 185%).

Availability of Data and Materials
The experimental data can be obtained through email communication with the author at sabry_fayed@eng.kfs.edu.eg.

Declarations

Ethics Approval and Consent to Participate
Not applicable.

Informed Consent
Informed consent was obtained from all individual participants included in this study.

Consent for Publication
All the authors agree that the article will be published after acceptance.

Competing Interests
The author declares that they have no competing interests.

References
Abed, F., el Refai, A., & Abdalla, S. (2019). Experimental and finite element investigation of the shear performance of BFRP-RC short beams. *Structures, 20*, 689–701.

Abed, F., Al-Mimar, M., & Ahmed, S. (2021). Performance of BFRP RC beams using high strength concrete. *Composites Part c: Open Access, 4*, 100107.

Abushanab, A., Alnahhal, W., & Farraj, M. (2021). Structural performance and moment redistribution of basalt FRC continuous beams reinforced with basalt FRP bars. *Engineering Structures, 240*, 112390.

Al-Abdwais, A., & Al-Mahaidi, R. (2016). Bond behaviour between NSM CFRP laminate and concrete using modified cement-based adhesive. *Construction and Building Materials, 127*, 284–292.

Al-Hamrani, A., Alnahhal, W., & Elahtem, A. (2021). Shear behavior of green concrete beams reinforced with basalt FRP bars and stirrups. *Composite Structures, 277*, 114619.

Al-Mahmoud, F., Castel, A., François, R., & Tourneur, C. (2011). Anchorage and tensionstiffening effect between near-surface-mounted CFRP rods and concrete. *Construction and Building Materials, 33*, 246–352.

Al-Obaidi, S. M., Saeed, Y. M., & Rad, F. N. (2018). Pullout Tests on Near-Surface-Mounted CFRP Rods with and Without Lateral Grooves. *International Journal of Engineering & Technology, 7*, 72.

Attia, K., el Refai, A., & Alnahhal, W. (2020). Flexural behavior of basalt fiber-reinforced concrete slab strips with BFRP bars: Experimental testing and numerical simulation. *Journal of Composites for Construction, 24*, 04020007.

Barros, J. A. and J. Sena-Cruz. Bond behavior of carbon laminate strips into concrete by pullout-bending tests. Bond in concrete: from research to standards: proceedings of the third International Symposium on Bond in Concrete. 2002.

Capozucca, R., Blasi, M. G., & Corina, V. (2015). NSM technique: Bond of CFRP rods and static/dynamic response of strengthened RC beams. *Composite Structures, 127*, 466–479.

Cruz, J. M. S., & Barros, J. A. O. (2004a). Bond between near-surface mounted carbon-fiber reinforced polymer laminate strips and concrete. *Journal of Composites for Construction, 8*, 519–527.

Cruz, J. M. S., & Barros, J. A. O. (2004b). Bond between near-surface mounted carbon-fiber-reinforced polymer laminate strips and concrete. *Journal of Composites for Construction, 8*, 519–527. https://doi.org/10.1061/(ASCE)1090-0268(2004)8

Data sheet of Sikadur 31CF, https://lbn.sika.com/dms/getdocument.get/3768ebb4-85cc-3ed5-b870-764a2dc4854e/Sikadur%20-31CF.pdf

De Lorenzis, L., & Nanni, A. (2001). Characterization of FRP rods as near-surface mounted reinforcement. *Journal of Composites for Construction, 5*(2), 114–121.

De Lorenzis, L., & Teng, J. G. (2007). Near-surface mounted FRP reinforcement: An emerging technique for strengthening structures. *Composites Part B Engineering, 38*, 119–143.

Dong Z, Wu G, Zhu H, Wei Y, Zhao XL, Shao X (2021) Bond and flexural performance of basalt fiber–reinforced polymer bar–reinforced seawater sea sand glass aggregate concrete beams. *Advances in Structural Engineering*, *24*(15), 3359–3374.

El Refai, A., Alnahhal, W., Al-Hamrani, A., & Hamed, S. (2022). Shear performance of basalt fiber-reinforced concrete beams reinforced with BFRP bars. *Composite Structures, 288*, 115443.

Elmesalami, N., Abed, F., & el Refai, A. (2021). Concrete columns reinforced with GFRP and BFRP bars under concentric and eccentric loads: Experimental testing and analytical investigation. *Journal of Composites for Construction, 25*, 04021003.

Elmessalami, N., el Refai, A., & Abed, F. (2019). Fiber-reinforced polymers bars for compression reinforcement: A promising alternative to steel bars. *Construction and Building Materials, 209*, 725–737.

Emara, M., Barris, C., Baena, M., Torres, L., & Barros, J. (2018). Bond behavior of NSM CFRP laminates in concrete under sustained loading. *Construction and Building Materials, 177*, 237.

Fayed, S., et al. (2023). Improving bond performance of ribbed steel bars embedded in recycled aggregate concrete using steel mesh fabric confinement. *Construction and Building Materials, 369*, 130452.

Gomez, J., Barris, C., Jahani, Y., Baena, M., & Torres, L. (2021). Experimental study and numerical prediction of the bond response of NSM CFRP laminates in RC elements under sustained loading. *Construction and Building Materials, 288*, 123082.

Kalupahana, W. K. K. G., Ibell, T. J., & Darby, A. P. (2013). Bond characteristics of near surface mounted CFRP bars. *Construction and Building Materials, 43*, 58–68. https://doi.org/10.1016/j.conbuildmat.2013.01.021

Lee, D., Cheng, L., & Yan-Gee Hui, J. (2013a). Bond characteristics of various NSM FRP reinforcements in concrete. *Journal of Composites for Construction, 17*, 117–129.

Lee, D., Cheng, L., & Yan-Gee Hui, J. (2013b). Bond characteristics of various NSM FRP reinforcements in concrete. *Journal of Composites for Construction, 17*, 117–129. https://doi.org/10.1061/(asce)cc.1943-5614.0000318

Liu, S., Wang, X., Ali, Y. M. S., Su, C., & Wu, Z. (2022). Flexural behavior and design of underreinforced concrete beams with BFRP and steel bars. *Engineering Structures, 263*, 114386.

Novidis, D. G., & Pantazopoulou, S. J. (2008). Bond tests of short NSM-FRP and steel bar anchorages. *Journal of Composites for Construction, 12*(3), 323–333.

Novidis, D. G., Pantazopoulou, S. J., & Tentolouris, E. (2007). Experimental study of bond of NSM-FRP reinforcement. *Construction and Building Materials, 21*(8), 1760–1770.

Peng, H., Hao, H., Zhang, J., Liu, Y., & Cai, C. S. (2015). Experimental investigation of the bond behavior of the interface between near-surface-mounted CFRP strips and concrete. *Construction and Building Materials, 96*, 11–19.

Sharaky, I. A., Torres, L., Baena, M., & Mi`as, C. (2013). An experimental study of different factors affecting the bond of NSM FRP bars in concrete. *Composite Structures, 99*, 350–365.

Soliman, S. M., El-Salakawy, E., & Benmokrane, B. (2011a). Bond performance of near surface mounted FRP bars. *Journal of Composites for Construction, 15*, 103–111.

Soliman, S. M., El-Salakawy, E., & Benmokrane, B. (2011b). Bond performance of near surface mounted FRP bars. *Journal of Composites for Construction, 15*, 103–111.

Teng, J. G., De Lorenzis, L., Wang, B., Li, R., Wong, T. N., & Lam, L. (2006). Debonding failures of RC beams strengthened with near surface mounted CFRP strips. *Journal of Composites for Construction, 10*(2), 92–105.

Tomlinson, D., & Fam, A. (2015). Performance of concrete beams reinforced with basalt FRP for flexure and shear. *Journal of Composites for Construction, 19*, 04014036.

Torres, L., Sharaky, I. A., Barris, C., & Baena, M. (2016). Experimental study of the influence of adhesive properties and bond length on the bond behaviour of NSM FRP bars in concrete. *Journal of Civil Engineering and Management, 22*, 808–817.

Wang, X., & Cheng, L. (2021a). Bond characteristics and modeling of near-surface mounted CFRP in concrete. *Composite Structures, 255*, 113011.

Wang, X., & Cheng, L. (2021b). Bond characteristics and modeling of near-surface mounted CFRP in concrete. *Composite Structures, 255*, 113011.

Wang, X., & Cheng, L. (2021c). Bond characteristics and modeling of near-surface mounted CFRP in concrete. *Composite Structures, 255*, 113011. https://doi.org/10.1016/j.compstruct.2020.113011

Wang, X., & Cheng, L. (2021d). Bond characteristics and modeling of near-surface mounted CFRP in concrete. *Composite Structures*. https://doi.org/10.1016/j.compstruct.2020.113011

Wang, X., Liu, S., Shi, Y., Wu, Z., & He, W. (2022). Integrated High-Performance Concrete Beams Reinforced with Hybrid BFRP and Steel Bars. *Journal of Structural Engineering, 148*, 04021235.

Zhu, Z., Zhu, E., & Chen, Z. (2018). the experiment analysis of bonding performance between near surface mounted CFRP strip and concrete at different curing temperatures, Urban Rail. *Transit, 4*, 155–162.

Publisher's Note

Sabry Fayed: Associate Professor, Department of Civil Engineering, Faculty of Engineering, Kafrelsheikh University, Kafrelsheikh, Egypt.

Emrah Madenci: Associate Professor, Department of civil engineering, Necmettin Erbakan University, 42090 Konya, Turkey.

Yasin Onuralp Özkiliç: Associate Professor, Department of civil engineering, Necmettin Erbakan University, 42090 Konya, Turkey.

Mohamed H. Zakaria: Assistant Professor, Department of Civil Engineering, Faculty of Engineering, Kafrelsheikh University, Kafrelsheikh, Egypt.